An analytical representation of the ground potential energy surface ($^2A'$) of the $H+Cl_2 \rightarrow HCl+Cl$ and $Cl+HCl \rightarrow HCl+Cl$ reactions, based on *ab initio* calculations

Miguel González,[a] J. Hijazo, J. J. Novoa, and R. Sayós[b]
Departament de Química Física, Facultat de Quimica, Universitat de Barcelona, Martí i Franquès, 1, 08028 Barcelona, Spain

(Received 26 August 1997; accepted 14 November 1997)

In this work we have studied at an *ab initio* level the lowest $^2A'$ potential energy surface (PES) of the HCl_2 system. This PES is involved in the $H(^2S)+Cl_2(X\ ^1\Sigma_g^+) \rightarrow HCl(X\ ^1\Sigma^+)+Cl(^2P)$ and $Cl(^2P)+HCl(X\ ^1\Sigma^+) \rightarrow HCl(X\ ^1\Sigma^+)+Cl(^2P)$ gas phase elementary chemical reactions. The former reaction is an important chemical laser while the second one is the most frequently used prototype of heavy–light–heavy reaction. A large number of points on the $^2A'$ PES have been calculated at the PUMP2/6-311G($3d2f$,$3p2d$) *ab initio* level. The *ab initio* calculations show the existence of two angular transition states with negligible or very small barriers to collinearity. This and other properties of the PES are in agreement with previous studies. An analytical expression based on a many-body expansion has been used to obtain a satisfactory fit of the 740 *ab initio* points calculated, with a root-mean-square deviation within the range of the estimated *ab initio* method error margin. This analytical representation of the $^2A'$ PES has been used to evaluate the variational transition state theory thermal rate constants of the above-mentioned reactions, including also the Cl+DCl reaction, and quite good agreement has been obtained when comparing with experimental results. The analytical PES obtained in this work is suitable for use in studies on the kinetics and dynamics of the HCl_2 system. © *1998 American Institute of Physics.* [S0021-9606(98)02207-7]

I. INTRODUCTION

The gas phase reactions

$$H(^2S)+Cl_2(X\ ^1\Sigma_g^+) \rightarrow HCl(X\ ^1\Sigma^+)+Cl(^2P), \quad \Delta E=-48.51 \text{ kcal mol}^{-1} \tag{1}$$

and

$$Cl(^2P)+HCl(X\ ^1\Sigma^+) \rightarrow HCl(X\ ^1\Sigma^+)+Cl(^2P), \quad \Delta E=0 \text{ kcal mol}^{-1} \tag{2}$$

have played and still are playing an important role in the field of reaction dynamics. The reaction energy (ΔE), equal to the difference between the diatomic dissociation energy (D_e) of reactants and products, has been derived from spectroscopic data.[1] Reaction (1) is a chemical laser and belongs to the hydrogen atom plus halogen molecule reactions family, which have been used to establish many of the earliest and most important hypotheses of reaction dynamics. Reaction (2) is the most frequently considered prototype of a reaction involving the transference of a light atom between two heavy ones [heavy–light–heavy (HLH) reactions]. We will consider briefly the most recent and reliable experimental and theoretical results reported for both reactions.

Reaction (1) has been the object of many experimental works. Thus, several important properties have been determined: thermal rate constant,[2,3] HCl vibrational and rotational distributions,[4–10] and DCl angular and velocity distributions.[11] Also, some attention has been payed to the *ab initio* characterization of the transition state.[12–14]

Geometries of the stationary points and barrier heights for reactions (1) and (2) have been calculated[13] employing *ab initio* methods and large basis sets with extensive treatment of electron correlation. The HCl_2 system has a slightly bent transition state (TS) with a very small barrier to collinearity, and the ClHCl system has a strongly bent TS around 140°, but the bending potential is rather flat and therefore the predicted barrier heights for the bent TS are quite similar to those obtained for the collinear arrangement. The most accurate results reported in Ref. 13 are consistent with the experimental barrier estimates for both reactions. Relativistic effects do not significantly influence the properties of the stationary points (assumed to be collinear).[14]

Reaction (2) has been the object of much less experimental work than reaction (1). Thus, only kinetics data[15–18] and transition state probing by negative ion photodetachment[19] have been reported. However, from a theoretical point of view more interest has been devoted to reaction (2) than to reaction (1), with different methodologies being applied, including *ab initio* methods (transition state characterization),[13,14,18] variational transition state rate theory (rate constant),[18] quasiclassical trajectories,[20–22] and quantum-mechanical approaches,[23–25] also taking into account the influence of atomic fine structure on the rate constant.[26,27] Moreover, for this reaction a London–Eyring–Polamyi–Sato (LEPS) empirical surface quite adequate to reproduce the kinetics data [hereafter referred to as the Bondi–Connor–Manz–Römelt (BCMR) surface] has been reported[28] and widely used in studies on the dynamics.

As mentioned above, when dealing with reaction (1) the general properties of the TS of reaction (2) have also been

[a]Electronic mail: miguel@dynamics.qf.ub.es
[b]Electronic mail: r.sayos@dynamics.qf.ub.es

indicated. The *ab initio* studies on reaction (2) have been mainly centered on the characterization of the transition state,[13,14,18] but in Ref. 27 analytical fittings were also provided for the three lowest potential energy surfaces (PESs) of the system ($1\,^2A'$, $2\,^2A'$, and $1\,^2A''$).

The variational transition state rate theory (VTST),[18] the quasiclassical trajectory (QCT) method,[20–22] and several quantum-mechanical (QM) approaches[23–27] have been applied to theoretically describe the kinetics and dynamics of the Cl+HCl reaction using different analytical potential energy surfaces (PESs). With the exception of the PES based on *ab initio* calculations used in Ref. 27, the PESs were derived from kinetics data or by combining this type of information with quite limited *ab initio* calculations mainly centered around the TS geometry.

This work complements previous contributions and the main goal of it is to derive an analytical expression from *ab initio* calculations for the lowest PES of the HCl_2 system, taking into account reactions (1) and (2). The paper is organized as follows. Section II shows the *ab initio* calculations and the fitting procedure of the $HCl_2(^2A')$ PES and a comparison with previous studies. Section III shows the VTST thermal rate constant calculations for the new analytical PES and a comparison with experimental results and earlier theoretical data. Finally, in Sec. IV the concludings remarks are given.

II. POTENTIAL ENERGY SURFACE

A. *Ab initio* calculations

In C_s symmetry, the most relevant symmetry for theoretical studies on the kinetics and dynamics of reactions (1) and (2), there is a single PES ($^2A'$ symmetry) correlating with $H(^2S)+Cl_2(X\,^1\Sigma_g^+)$ and there are three PESs $[(2)^2A' + {}^2A'']$ correlating with $Cl(^2P)+HCl(X\,^1\Sigma^+)$. Hence, both asymptotes may correlate through one of the $^2A'$ PES. As will be shown below, from the *ab initio* calculation it turns out that the lowest $^2A'$ PES correlates both asymptotes. This result was also obtained in previous works.[13,27]

Although there exists a very recent *ab initio* study,[27] involving the three lowest PESs of the system ($1\,^2A'$, $2\,^2A'$, and $1\,^2A''$) at a multiconfiguration self-consistent field (MCSCF) level, in the present contribution we have paid particular attention to earlier *ab initio* calculations,[13] where higher levels of the theory were considered for the lowest PES ($1\,^2A'$).

We have carried out an *ab initio* study on the ground $^2A'$ PES of this system. This work has allowed us to characterize the properties of the stationary points and to calculate a large number of points of the PES. We have selected a suitable method and basis set to calculate a large number of *ab initio* points, accurate enough to be used in the construction of analytical representations of the lowest $^2A'$ PES. From Ref. 13, where different *ab initio* methods to deal with electron correlation and basis sets were used, it comes out that the $HCl_2(^2A')$ wave function is mostly single determinantal in nature at all the stationary points of the PES, and the unrestricted second-order Møller–Plesset (UMP2) method is, in principle, accurate enough. Thus, the set of *ab initio* points of the PES required to be used in the fitting of an analytical expression suitable for reaction dynamics studies have been calculated at the projected unrestricted second-order Møller–Plesset level (PUMP2) using a large basis set [6-311G $(3d2f,3p2d)$ basis set], PUMP2/6-311G$(3d2f,3p2d)$ *ab initio* level hereafter, by means of the GAUSSIAN 94 package.[29] The PUMP2 method has been chosen to eliminate the small spin contaminations which have appeared in some regions of the PES, mainly in the dissociation plateau, $H(^2S)+Cl(^2P)+Cl(^2P)$, and transitions states: $\langle S^2\rangle = 0.818$ and 0.798 for H–Cl–Cl (TS1) and Cl–H–Cl (TS2), respectively, and $\langle S^2\rangle = 0.818-0.872$ and 0.803–0.783 for H–Cl–Cl (180°–120°) and Cl–H–Cl (180°–80°) barriers. In the dissociation plateau, however, the spin contamination is due to the degeneracy of both the doublet and quadruplet states generated and thus the energy is not affected. But, in the second case the spin contamination of the unrestricted Hartree–Fock (UHF) wave function arises from a crossing between two different states and affects the energy values.

The stationary points [reactants, products, and transition states for both reactions (TS1 and TS2)] on the $^2A'$ PES have been located and characterized (geometry, energy, and harmonic frequencies) using standard procedures (analytical gradients are available at the UMP2 level while for the PUMP2 method the stationary points have been obtained using splines). Table I gives the properties of the stationary points at the PUMP2/6-311G$(3d2f,3p2d)$ and UMP2/6-311G$(3d2f,3p2d)$ *ab initio* levels. The PUMP2 geometry of the transition states have been obtained by interpolation within a grid of *ab initio* points calculated around the region where the TSs are located. The harmonic frequencies are only reported at the UMP2/6-311G$(3d2f,3p2d)$ level, where analytical gradients are available. From Table I it turns out that the most important differences between the PUMP2 and UMP2 methods occur for the energy barriers, which are substantially lower in the former case. Thus, the PUMP2 energy barriers for reactions (1) and (2) are equal to 0.55 and 5.94 kcal mol^{-1}, respectively, while the corresponding UMP2 values are 1.41 and 8.53 kcal/mol^{-1}, respectively.

In the next paragraphs the present *ab initio* results will be compared with experimental data and with the *ab initio* results obtained in Ref. 13 taking into account the best levels of the theory considered: multireference singles and doubles configuration interaction method with Davidson correction (MRCI/D method), PUMP2/6-311G$(2df,2pd)$ at the optimal geometries given by UMP2/6-311G$(2d,2p)$ (method III//I), PUMP2/6-311G$(2df,2pd)$ (method III), PUMP2/6-311G$(2df,2pd)$ with an extrapolation procedure (SAC method). In the MRCI calculations a basis set of $14s11p3d1f$ contracted to $11s9p3d1f$ was employed for Cl and a basis set of $6s2pd$ was used for H. In what respects to the Møller–Plesset formulation used in Ref. 13, including also the case of the spin projected form, only at the UMP2/6-311G$(2d,2p)$ level (method I) the inner shells were correlated.

The present *ab initio* results (distance, dissociation energy, and harmonic frequency) for the diatomic molecules are in very good agreement with the experimental data[1]

TABLE I. Properties of the stationary points of the ground $(^2A')HCl_2$ PES and features of the analytical representation.[a]

Stationary point	R_{HCl} (Å)	R_{ClCl} (Å)	<HClCl (°) <ClHCl (°)	E(kcal mol^{-1})[b]	ν_i (cm^{-1})		
$H(^2S)+Cl_2(X\ ^1\Sigma_g^+)$[c]							
PUMP2	⋯	1.9939	⋯	0.0		571.1	
Analytical representation[d]		1.9939	⋯	0.0		580.2	
Experimental		1.988		0.0		559.7	
TS1 (HClCl)							
PUMP2	2.1159	2.0035	175.03	0.55	943.3*i*	77.6	636.6[e]
Analytical representation[d]	2.2395	1.9849	180.00	0.29	220.3*i*	101.2	672.5
BCMR surface	2.7091	1.9903	180.00	0.37	183.2*i*	14.0	552.3
$Cl(^2P)+HCl(X\ ^1\Sigma^+)$[c]							
PUMP2	1.2687	⋯	⋯	−49.46		3036.0	
Analytical representation[d]	1.2687	⋯	⋯	−49.46		3060.4	
Experimental	1.275			−48.51		2990.9	
TS2 (ClHCl)							
PUMP2	1.4698	2.7277	136.23	−43.52	1673.9*i*	210.5	1195.5[e]
Analytical representation[d]	1.4679	2.9793	141.06	−41.88	348.6*i*	166.3	1092.0
BCMR surface	1.4666	2.9332	180.00	−39.94	1399.3*i*	508.7	343.8

RMSD (eV) of the fitted *ab initio* points

	RMSD	Points
MEP[f]	0.1187	29
$E<E$ (reactants)	0.1749	409
Total	0.1661	740

[a]PUMP2 results correspond to the PUMP2/6-311G($3d2f$,$3p2d$) *ab initio* results, the BCMR LEPS surface is reported in Ref. 28, and the experimental data have been taken from Ref. 1.

[b]Zero of energy taken in $H+Cl_2$. Energies do not include the vibrational zero point energy. *Ab initio* energy of $H+Cl_2$: −919.999 103 h (PUMP2 and UMP2).

[c]The dissociation energies of Cl_2 and HCl, given in the order PUMP2, UMP2 and experimental (Ref. 1), are equal to 2.4674, 2.5735, and 2.5143 eV, and 4.6125, 4.6655, and 4.6172 eV, respectively.

[d]Optimal analytical representation based on a many-body expansion to fit the PUMP2 *ab initio* points (see the text).

[e]Harmonic frequencies at the UMP2 level of the antisymmetric stretching, bending, and symmetric stretching vibrational modes, respectively.

[f]Minimum energy path (IRC).

(Table I), and the geometry, barrier height, and harmonic frequencies of both transition states are in good agreement with previously reported results for TS1[12–14] and TS2.[13,14,18] The energy barriers are also close to the ones of the BCMR PES,[28] although the *ab initio* calculations predict the existence of bent (H–Cl–Cl) and strongly bent (Cl–H–Cl) transition states, in contrast with what happens in the BCMR case where both TS are linear. However, the *ab initio* barrier to collinearity is negligible for TS1 and less than 1 kcal mol^{-1} for TS2.

The TS1 geometry obtained agrees quite well with the *ab initio* results reported in Ref. 13. Thus, the MRCI/D TS1 occurs at $R_{HCl}=1.931$ Å and $R_{ClCl}=2.096$ Å (only collinear geometries were considered), while the corresponding UMP2 6-311G($2d$,$2p$) distances reported are 1.866 and 2.054 Å, respectively, with a HClCl angle of 169.3°.[13] The barrier to collinearity is extremely small (0.1 kcal mol^{-1}). Thus, as in the present calculations at the PUMP2 level, both levels of the theory (MRCI/D and UMP2) predict that TS1 is located rather early in the reactants valley. In the present work, the UMP2 TS1 geometry is very close to the PUMP2 one, although the PUMP2 R_{HCl} distance is about 13% larger than UMP2 value (cf. Table I). TS1 harmonic frequencies were not reported in Ref. 13, although the zero point energy obtained from method I, 1.13 kcal mol^{-1}, is very close to the one obtained here (1.02 kcal mol^{-1}).

The energy barrier for reaction (1) obtained here (0.55 kcal mol^{-1}) is substantially lower than the values reported in Ref. 13, and after the addition of the zero point energy (ZPE) to the PUMP2 6-311G($3d2f$,$3p2d$) energy barrier, taking into account the UMP2 6-311G($3d2f$,$3p2d$) harmonic frequencies, a value of 0.75 kcal mol^{-1} results. This value is consistent with the experimental activation energy value ($1.2_0\pm0.1_4$ kcal mol^{-1} ($T=252-458$ K)[2] and $1.1_5\pm0.1_2$ kcal mol^{-1} ($T=300-730$ K)[3]). In respect to Ref. 13, the MRCI/D barrier is 1.65 kcal mol^{-1}, while the UMP2 6-311G($2df$,$2pd$)//UMP2 6-311G($2d$,$2p$) barrier after spin projection (there is some spin contamination at TS1, $\langle S^2\rangle=0.84$) is reduced to 2.24 kcal mol^{-1}. The MRCI/D results and the III//I ones reported in Ref. 13, after correction of the energy barrier with the ZPE derived from the UMP2 6-311G($2d$,$2p$) harmonic frequencies, are equal to 1.98 and 2.57 kcal mol^{-1}, respectively.

The TS2 geometry obtained here (Table I) also agrees

quite well with the *ab initio* results reported in Ref. 13. Thus, the TS2 occurs at C_{2v} symmetry with a R_{HCl}(Å) [ClHCl angle (°)] equal to 1.494, 1.485, 1.484, and 1.482 (148, 137, 145, and 142) respectively, for the MRCI/D, III//I, III and SAC *ab initio* methods,[13] while in the present work the next set of values are obtained for the distance and angle at the PUMP2 level: 1.4698 Å and 136.23°, respectively. The UMP2 saddle point geometry is close to the PUMP2 one and all levels of the theory predict a C_{2v} TS2. TS2 harmonic frequencies obtained here at the UMP2 6-311G($3d2f$, $3p2d$) level (Table I) agree quite well with those reported in Ref. 13 [UMP2 6-311G($2d$,$2p$) level (method I), $\nu_{\mathrm{s.s.}}=1168$, $\nu_b=204$, $\nu_{\mathrm{a.s.}}=1905i(\mathrm{cm}^{-1})$].

The energy barrier obtained here, 5.94 kcal mol^{-1} at the PUMP2 6-311G($3d2f$,$3p2d$) level [3.61 kcal mol^{-1} if the UMP2 6-311G($3d2f$,$3p2d$) ZPE is included], is consistent with the experimental activation energy value [$5.5\pm(0.2$–$2.5)$ kcal mol^{-1} ($T=312.5$–423.2 K)[18]]. The energy barrier for reaction (2) reported in Ref. 13 is substantially larger than the one obtained here, although their reported values are also consistent with experimental data. Thus, the MRCI/D, III//I, III, and SAC results, after correction of the energy barrier with the ZPE derived from the UMP2 6-311G($2d$,$2p$) harmonic frequencies, are equal to 7.68, 6.49, 6.68, and 5.30 kcal mol^{-1}, respectively.

It is worth noting that relativistic effects do not significantly influence the collinear stationary points of reactions (1) and (2).[14] In fact, a MP2 study shows that scalar relativistic effects have little influence on the geometries and energies of these points. For reaction (1), spin–orbit interaction has no influence on the barrier energy but increases the reaction energy. The total relativistic effect is an increase of the reaction energy by 0.55 kcal mol^{-1}. For reaction (2) the barrier decreases by 0.12 kcal mol^{-1} due to scalar relativistic effects, but this very small decrease is counterbalanced by an increase of 0.60 kcal mol^{-1} due to spin–orbit interaction, resulting in a total relativistic barrier increase of 0.48 kcal mol^{-1}.

To explore the regions of the PES relevant to the kinetics and dynamics a total amount of 740 points (geometries) have been considered for the $^2A'$ PES at the PUMP2/6-311G($3d2f$,$3p2d$) *ab initio* level, arranged in the following way: (a) TS of reactions (1) and (2); (b) minimum energy path (MEP) of reaction (1) using the intrinsic reaction coordinate (IRC) method;[30] (c) dependence of the barrier height with the attack angle (HClCl′ and ClHCl′ angles between 180° and 80°); (d) small networks of points (around 30 points) centered in the geometry barriers; (e) bending energy curves for the H–Cl–Cl and Cl–H–Cl arrangements, considering the two distances fixed to values of the corresponding TS. Moreover, 20 and 24 points have also been calculated, respectively, for the Cl_2 and HCl energy curves, to obtain a fully *ab initio* surface for this system. The calculation of each triatomic point takes about 1 h on an IBM RS/6000 7030 3BT workstation.

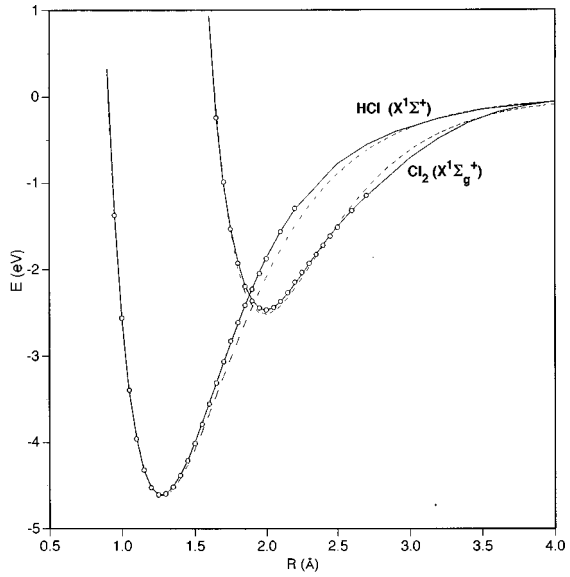

FIG. 1. Potential energy curves of the $Cl_2(X\ ^1\Sigma_g^+)$ and $HCl(X\ ^1\Sigma^+)$ diatomic molecules. The fits of the diatomic *ab initio* points employed in the analytical PES derived in this work are shown by continuous lines, and the Morse diatomic curves employed in the BCMR empirical PES are indicated by dashed lines.

B. Analytical fit

A many-body expansion[31] has been employed to derive an analytical expression for the ground ($^2A'$) HCl_2 potential energy surface, which can be written as

$$V_{\mathrm{HClCl'}}(R_1,R_2,R_3)=V_{\mathrm{H}}^{(1)}+V_{\mathrm{Cl}}^{(1)}+V_{\mathrm{Cl'}}^{(1)}+V_{\mathrm{HCl}}^{(2)}(R_1)+V_{\mathrm{ClCl'}}^{(2)}(R_2)+V_{\mathrm{HCl'}}^{(2)}(R_3)+V_{\mathrm{HClCl'}}^{(3)}\times(R_1,R_2,R_3), \tag{3}$$

where $V^{(2)}$ and $V^{(3)}$ are the two-body and three-body terms, respectively, and R_1, R_2, and R_3 are the HCl, ClCl′, and HCl′ distances, respectively. In this equation, the monoatomic terms $V^{(1)}$ have been omitted because all possible reaction channels for $H(^2S)+Cl_2(X\ ^1\Sigma_g^+)$ and $Cl(^2P)+HCl(X\ ^1\Sigma^+)$ correlate with the atoms in their ground electronic states: $H(^2S)+Cl(^2P)+Cl(^2P)$.

Extended-Rydberg potentials up to the fifth order have been used to describe the two-body interactions (diatomic potential energy curves) in Eq. (3), for the $Cl_2(X\ ^1\Sigma_g^+)$ and $HCl(X\ ^1\Sigma^+)$ diatomic curves:

$$V^{(2)}(R)=-D_e(1+a_1\rho+a_2\rho^2+a_3\rho^3+a_4\rho^4+a_5\rho^5)e^{-a_1\rho}, \tag{4}$$

where D_e and R_e are the dissociation energy and the equilibrium bond length of the diatomic molecule, respectively, and ρ is defined as being equal to $R-R_e$. The parameters a_i have been determined by means of a nonlinear least-squares procedure,[32] taking into account the corresponding *ab initio* points (20 and 24 points for Cl_2 and HCl, respectively). Figure 1 shows both the PUMP2/6-311G($3d2f$,$3p2d$) *ab initio* data and fitted energy curves of the two diatomics involved in reactions (1) and (2). From Figure 1 it turns out that a very good fitting of the diatomic *ab initio* points has been obtained. The root-mean-square deviation (RMSD) for the di-

TABLE II. Optimal parameters for the extended-Rydberg functions of the *ab initio* diatomic potential energy curves.

Molecule	D_e (eV)	R_e (Å)	a_1 (Å^{-1})	a_2 (Å^{-2})	a_3 (Å^{-3})	a_4 (Å^{-4})	a_5 (Å^{-5})
$Cl_2(X\ ^1\Sigma_g^+)$	2.4673	1.9939	5.2714	9.5082	9.5665	13.0256	18.4929
$HCl(X\ ^1\Sigma^+)$	4.6123	1.2687	3.6314	2.9360	1.0346	−0.8237	1.6907

atomic energy curves of Cl_2 and HCl, are 0.888×10^{-2} and 0.943×10^{-2} eV, respectively. The optimal extended-Rydberg parameters of each molecule are given in Table II. In Fig. 1 the Morse diatomic curves used in the BCMR LEPS surface have also been plotted. In general these curves are quite close to the corresponding extended-Rydberg ones.

The three-body term consists of a fifth-order polynomial expressed in terms of three variables ρ_i, $\rho_i=R_i-R_i^0$, where the reference structure (R_1^0,R_2^0,R_3^0) has been taken as a C_{2v} structure located between both equivalent UMP2 TS1 structures resulting from interchanging the Cl atoms $(R_1^0=R_3^0=0.5\ (R_{1,\mathrm{TS1}}+R_{3,\mathrm{TS1}})=3.1157$ Å; $R_2^0=R_{2,\mathrm{TS1}}=2.0035$ Å), and a range function $T(R_1,R_2,R_3)$ which cancels the three-body term as one of the three atoms is separated from the other ones:

$$V_{ABC}^{(3)}(R_1,R_2,R_3)=P(\rho_1,\rho_2,\rho_3)T(\rho_1,\rho_2,\rho_3), \tag{5}$$

where

$$P(\rho_1,\rho_2,\rho_3)=V^0\left(1+\sum_{i,j,k=0}^{1\leqslant i+j+k\leqslant 5} c_{ijk}\rho_1^i\rho_2^j\rho_3^k\right), \tag{6}$$

with i, j, and k being positive integer numbers, and

$$T(\rho_1,\rho_2,\rho_3)=\prod_{i=1}^{3}\left[1-\tanh\left(\frac{\gamma_i\rho_i}{2}\right)\right]. \tag{7}$$

The 36 three-body parameters $(V^0,\{c_{ijk}\},\{\gamma_i\})$ different from zero (V^0, 33 c_{ijk} coefficients, γ_1, and γ_2), the remaining ones are zero due to the symmetry of the system, have been determined by a weighted nonlinear least-squares procedure[33] using the following PUMP2/6-311G$(3d2f,3p2d)$ *ab initio* data: (a) energy, geometry, and harmonic force constants of both *ab initio* TS, and (b) a total of 740 *ab initio* points within the above-mentioned triatomic geometrical arrangements and with energies up to 2.5 eV over reactants. The inclusion of points with higher energies worsened the adjustment and, in fact, is not necessary for the study of both reactions at the usual experimental conditions. Moreover, the energy barriers have been scaled to reproduce as closely as possible the experimental thermal rate constants for reactions (1) and (2), when these properties have been calculated using the variational transition state theory (see Sec. III). The energy barrier of the fitted PES was also scaled following the same procedure in a recent work of the present authors on the O+CS→CO+S chemical laser reaction.[34]

About 50 analytical representations of the lowest $^2A'$ PES have been carefully analyzed to obtain the best fitted surface. In a first stage of the fit, an initial guess for the γ_i parameters has been used and the corresponding optimal parameters of the polynomial have been obtained by a linear least-squares procedure. These parameters have later been used as input parameters in a nonlinear least-squares procedure that leads to several analytical PESs with smaller RMSD. In the last stage of the fitting procedure, a weighted nonlinear least-squares procedure has been considered, taking as starting points the parameters of the previous PES.[33] Weights different from 1.0 have been used at this stage, only for several *ab initio* points close to the TS, and for the energy and first partial derivatives (with respect to the HCl and ClCl′ interatomic distances and HClCl′ angle) at the transition states. This was necessary to scale the energy barriers of both reactions to the values finally selected.

Harmonic force constants at the transition states geometries have also been introduced in the fit by using small weights (about 0.1), because higher values greatly increased the RMSD of the *ab initio* points. During the fit, some additional *ab initio* points have also been calculated to better describe the regions of the surface where spurious minima appeared [e.g., in the HClCl and ClHCl collinear and ClHCl angular (103.7°) regions]. For the analytical surfaces considered, all important spurious minima have been removed and plots at different HClCl and ClHCl angles have been carefully analyzed. Spurious minima with deep energies lower than 1 kcal mol^{-1} have been considered negligible, and are common for the kind of analytical expression employed due to the polynomial term.

In Table III are shown the optimal three-body parameters of the lowest $^2A'$ PES. The properties of the stationary points on the fitted PES, together with those of the *ab initio* calculations and the BCMR surface are given in Table I. Even though very different initial parameters have been considered in the fitting procedure, there has been a clear convergence to the set of optimal parameters reported. Table I also includes the RMSD values for different regions of the PES. The RMSD value for the set of points with $E<E(\mathrm{H}+\mathrm{Cl}_2)$, RMSD=0.175 eV (409 points), is close to the one for the complete set of points, RMSD=0.166 eV (740 points), and the corresponding values for the minimum energy path (MEP) following the IRC method is lower but not far from the previous ones, RMSD=0.119 eV (29 points). In Fig. 2 the equipotential contour diagrams for this PES are presented for reactions (1) and (2) considering HClCl and ClHCl angles of 180° and 100°. The surface plots show a smooth fit of the *ab initio* data for each angle without spurious artifacts.

The stationary point properties derived from the fitted PES and the *ab initio* ones are in quite good agreement (Table I), taking into account that the energy barriers have been scaled to reproduce the rate constants of reactions (1) and (2) and the *ab initio* harmonic frequencies are given at the UMP2/6-311G$(3d2f,3p2d)$ level while the analytical representation fits PUMP2/6-311G$(3d2f,3p2d)$ *ab initio* points. The HClCl barrier has been lowered by 0.26 kcal mol^{-1} and the ClHCl one increased by

TABLE III. Optimal three-body parameters for the analytical representation of the ground ($^2A'$)HCl_2 PES.[a]

Parameter	Value	Parameter	Value	Parameter	Value
V^0	0.5840				
$R^0_{1,3}$	3.1157	R^0_2	2.0035		
γ_1	3.4515	γ_2	0.0000	γ_3	−2.2231
C_{100}	2.5087	C_{003}	0.8266	C_{401}	3.5828
C_{010}	0.0000	C_{400}	−4.4795	C_{320}	1.2858
C_{001}	0.4271	C_{310}	0.0000	C_{311}	0.0000
C_{200}	2.1554	C_{301}	−0.07202	C_{302}	2.7471
C_{110}	0.0000	C_{220}	3.0182	C_{230}	0.0000
C_{101}	−2.7115	C_{211}	0.0000	C_{221}	−0.9859
C_{020}	0.8954	C_{202}	13.0798	C_{212}	0.0000
C_{011}	0.0000	C_{130}	0.0000	C_{203}	−2.1040
C_{002}	−0.1140	C_{121}	0.4474	C_{140}	−0.07957
C_{300}	−8.2058	C_{112}	0.0000	C_{131}	0.0000
C_{210}	0.0000	C_{103}	1.1986	C_{122}	−0.4765
C_{201}	−16.3816	C_{040}	−0.02378	C_{113}	0.0000
C_{120}	0.8302	C_{031}	0.0000	C_{104}	−0.1497
C_{111}	0.0000	C_{022}	0.5000	C_{050}	0.0000
C_{102}	−0.5500	C_{013}	0.0000	C_{041}	−0.3974
C_{030}	0.0000	C_{004}	−0.5460	C_{032}	0.0000
C_{021}	0.6957	C_{500}	−0.4051	C_{023}	−0.6877
C_{012}	0.0000	C_{410}	0.0000	C_{014}	0.0000
				C_{005}	0.1198

[a]Units are: C_{ijk}/Å$^{-(i+j+k)}$, V^0/eV, γ_i/Å^{-1}, R^0_2/Å.

1.64 kcal mol^{-1}, while the ZPE are 2.07 and 1.80 kcal mol^{-1}, respectively. For reaction (1), the fitted ZPE differs from the *ab initio* value (1.02 and 2.01 kcal mol^{-1}, respectively) as in the fitted PES TS1 is collinear. The moduli of the fitted imaginary frequencies are 21%–23% of the *ab initio* values, and for TS1 it becomes quite close to the BCMR value.

In spite of the differences observed between the PES reported here and the earlier BCMR surface, the most remarkable ones occurring for reaction (1), it should be pointed out that, although the BCMR surface favors more a collinear approach of reactants (all LEPS surfaces exhibit collinear saddle points) than our analytical PES (collinear HClCl and bent ClHCl saddle points), the barrier energy of the PES derived in this work changes a little amount when a collinear instead of a bent approach or reactants is considered (Table IV). For reaction (1) the barrier increases less than 1 kcal mol^{-1} when the HClCl angle changes from 180° to 150°, while for reaction (2) the barrier is essentially the same when the ClHCl angle changes from 180° to 130°. On the other hand, the local behavior of the barrier energy and geometry around collinear arrangements of reactants is quantitatively very similar for both analytical PESs, except from what refers to $R_{\mathrm{HCl},b}$ of reaction (1) that is substantially larger in the BCMR case.

III. THERMAL RATE CONSTANTS

The thermal rate constants for reactions H+Cl_2→HCl+Cl (1), Cl+HCl→HCl+Cl (2), and Cl+DCl→DCl+Cl (3) have been calculated, within the 150–1000 K temperature range, using the variational transition state theory (VTST) with semiclassical tunneling, as implemented in the POLYRATE program.[35] VTST rate constants have been computed using the improved canonical variational theory (ICVT). Tunneling corrections have been taken into account by means of the small curvature tunneling semiclassical adiabatic ground state (ICVT/CD-SCSAG) method, and also using the microcanonical optimized multidimensional tunneling (ICVT/μOMT) method. Table V shows the rate constants at 300 and 500 K and Arrhenius parameters in the temperature ranges where the experimental measurements are available [252–730 K and 312.5–423.2 K for reactions (1) and (2)–(3), respectively], computed using the optimal analytical representation of the HCl_2($^2A'$) *ab initio* PES developed in Sec. II and the earlier BCMR empirical surface together with the experimental data. Figure 3 presents the theoretical and experimental Arrhenius plots. In Table V and Fig. 3 the rate constants and preexponential factors directly obtained in the calculations have been divided by three to obtain the correct rate constants for reactions (2) and (3) (see details below). In what follows, it will be shown that the VTST thermal rate constants calculated with the present PES give in general better agreement with the experimental rate constants than in the case of the earlier BCMR PES. For reaction (2), the present results will also be compared with approximate quantum mechanical data previously reported at a single surface[24] and multisurface[27] levels.

For the H+Cl_2 reaction, although the theoretical rate constants have been fitted according to the Arrhenius equation as in the experiments,[2,3] both the theoretical and experimental (expt.) Arrhenius plots present a clear curvature, with a very similar shape in the case of the ICVT/CD-SCSAG and ICVT/μOMT calculations performed on the PES obtained in this work and the experimental data. The error margins indicated in Table V for the theoretical activation energy (E_a) and preexponential factor (A) of reactions (1)–(3) arise from the curvature of the Arrhenius plot. For reaction (1) the ICVT/CD-SCSAG method yields the same results as the ICVT/μOMT one, the best VTST method considered here. For our PES the k(ICVT/μOMT)/k(ICVT) ratio is equal to 1.18 (1.04) and 1.06 (1.01) at 300 and 500 K, respectively, where as in what follows the BCMR values are between parentheses. The ratio k(ICVT/μOMT)/k(expt.) ranges from 0.53 (2.36) to 0.50 (1.90) in the 300–500 K T interval, while A(ICVT/μOMT)/A(expt.) and E_a(ICVT/μOMT)/E_a(expt.) are equal to 0.51 (1.50) and 1.00 (0.75), respectively. The direct comparison between the ICVT/μOMT data for the PES derived here with the ones arising from the BCMR surface leads to: k(present PES)/k(BCMR)=0.22–0.26 from 300 to 500 K, A(present PES)/A(BCMR)=0.34 and E_a(present PES)/E_a(BCMR)=1.33. From the above-mentioned results it comes out that our PES better describes the thermal rate constant of reaction (1), as it quantitatively reproduces the experimental E_a value and gives an A factor that is half the measured one, while the BCMR surface leads to E_a and A values that are respectively 50% higher and 25% lower than the corresponding experimental results.[2,3] Moreover, the shape of the corresponding ICVT/CD-SCSAG and ICVT/μOMT Arrhenius plot is more similar to the experiments than in the BCMR case.

As was indicated in Sec. II, under C_s symmetry there is

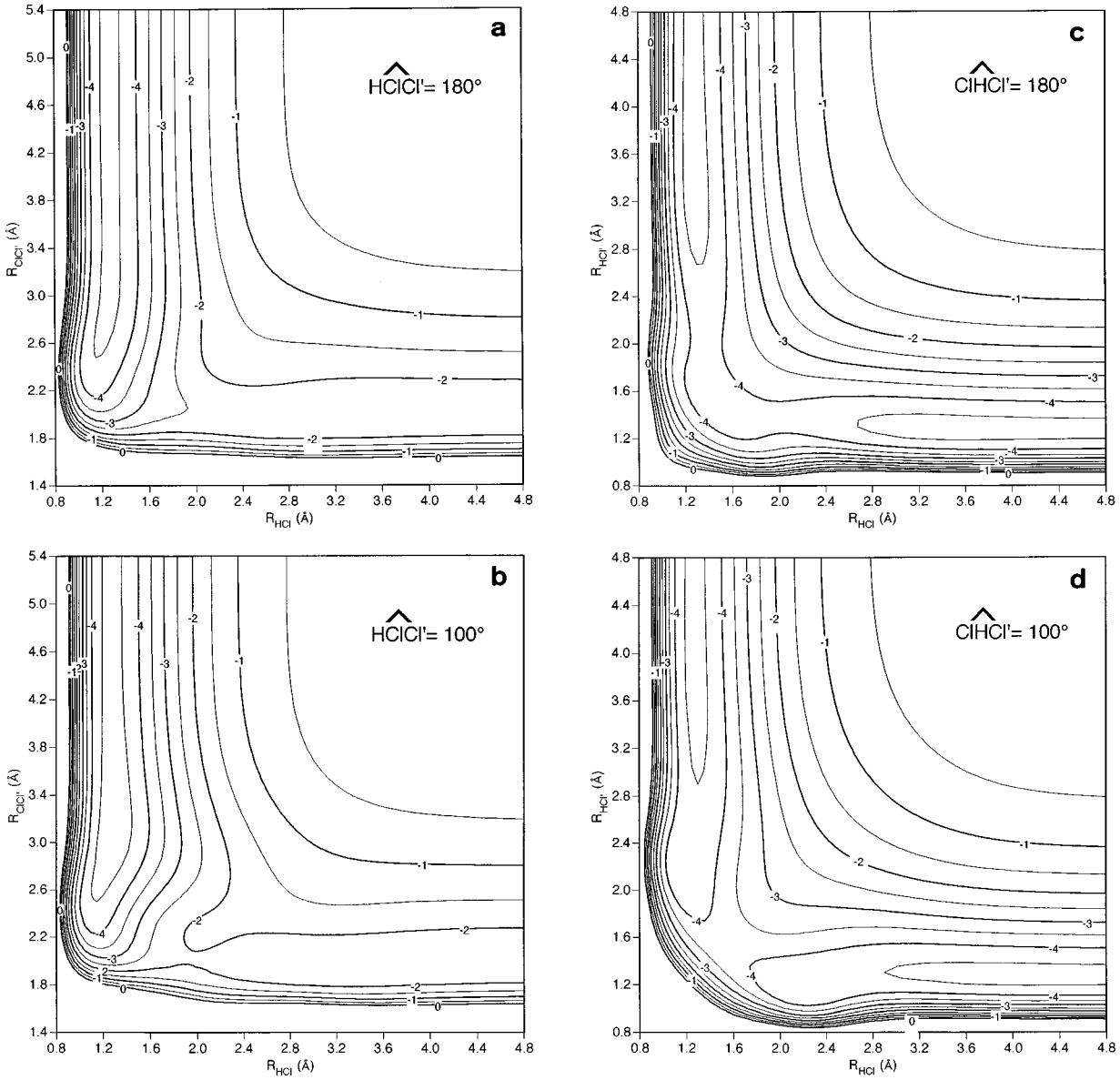

FIG. 2. Equipotential curves of the analytical ground state ($^2A'$) HCl_2 PES derived in this work at several angles: HClCl angle equal to 180° (a) and 100° (b); ClHCl angle equal to 180° (c) and 100° (d). The contours are given in 0.5 eV intervals and the zero of energy is taken in dissociated atoms.

a single PES ($^2A'$ symmetry) correlating with $H(^2S)+Cl_2(X\ ^1\Sigma_g^+)$ and there are three PESs ($(2)^2A'+^2A''$) correlating with $Cl(^2P)+HCl(X\ ^1\Sigma^+)$, both asymptotes being correlated through the lowest $^2A'$ PES. Thus, in the present VTST calculations it was assumed that among the three PESs that are degenerated in the Cl+HCl arrangement only the lowest $^2A'$ PES contributes to the reactivity in the interval of temperatures considered, and consequently a statistical multiplying factor equal to 1/3 has been included into the calculated rate constants and preexponential factors for reactions (2) and (3), which are given in Table V (see also Fig. 3). Of course, this means that we are neglecting the possible contribution to reactivity of electronically nonadiabatic processes involving the (2) $^2A'$ and 1 $^2A''$ PESs, but from the results obtained and taking into account the experimental error margins it seems that a single surface treatment based on the lowest $^2A'$ PES is accurate enough to account for the experimental rate constants.

TABLE IV. Angular dependence of the barrier energy and geometry for the optimal analytical representation of the $HCl_2(^2A')$ PES and the BCMR PES.

Angle (deg)	E_b (kcal mol^{-1})		$R_{HCl,b}$ (Å)		$R_{ClCl,b}$ (Å)	
	Present PES	BCMR	Present PES	BCMR	Present PES	BCMR
HClCl						
80	10.90	2.87	1.983	2.101	2.048	2.017
130	5.27	0.43	1.955	2.651	2.057	1.991
180	0.29	0.37	2.239	2.709	1.985	1.990
ClHCl						
80	40.70	58.18	1.722	1.783	2.213	2.292
130	7.89	14.35	1.475	1.498	2.673	2.716
180	7.99	8.57	1.466	1.467	2.934	2.933

For the Cl+HCl reaction the theoretical Arrhenius plots present a clear curvature, this is not observed in the measured ones due to the narrow interval of temperature considered in the experiments (312.5–423.2 K).[15,16,18] The ICVT/

TABLE V. VTST thermal rate constants and Arrhenius parameters for the present analytical ground $(^2A')HCl_2$ PES, BCMR PES, and experimental data.

	$(k_{500\,K}, k_{300\,K})$[a]		
	$H+Cl_2 \rightarrow HCl+Cl$	$Cl+HCl \rightarrow HCl+Cl$	$Cl+DCl \rightarrow DCl+Cl$
PES of this work[b]			
ICVT	$(2.01\times10^{-11},\ 8.71\times10^{-12})$	$(5.67\times10^{-14},\ 0.93\times10^{-15})$	$(2.47\times10^{-14},\ 2.87\times10^{-16})$
ICVT/CD-SCSAG	$(2.14\times10^{-11},\ 1.03\times10^{-11})$	$(5.93\times10^{-14},\ 1.05\times10^{-15})$	$(2.47\times10^{-14},\ 2.87\times10^{-16})$
ICVT/μOMT	$(2.14\times10^{-11},\ 1.03\times10^{-11})$	$(5.93\times10^{-14},\ 1.05\times10^{-15})$	$(2.42\times10^{-14},\ 2.71\times10^{-16})$
PES BCMR[b]			
ICVT	$(8.09\times10^{-11},\ 4.45\times10^{-11})$	$(1.06\times10^{-14},\ 1.15\times10^{-16})$	$(0.34\times10^{-14},\ 1.89\times10^{-17})$
ICVT/CD-SCSAG	$(8.20\times10^{-11},\ 4.63\times10^{-11})$	$(1.23\times10^{-14},\ 1.71\times10^{-16})$	$(0.45\times10^{-14},\ 0.40\times10^{-16})$
ICVT/μOMT	$(8.20\times10^{-11},\ 4.63\times10^{-11})$	$(4.13\times10^{-14},\ 1.78\times10^{-15})$	$(1.03\times10^{-14},\ 1.96\times10^{-16})$
Experimental[c]	$(4.31\times10^{-11},\ 1.96\times10^{-11})$	$(3.89\times10^{-14},\ 1.01\times10^{-15})$	$(1.37\times10^{-14},\ 1.08\times10^{-16})$
	ICVT/μOMT and experimental Arrhenius parameters[d]		
PES of this work[b]			
A	$(7.2\pm0.7)\times10^{-11}$	$(2.3\pm0.3)\times10^{-11}$	$(1.9\pm0.3)\times10^{-11}$
E_a	1.2 ± 0.1	6.0 ± 0.1	6.7 ± 0.1
PES BCMR[b]			
A	$(2.1\pm0.1)\times10^{-10}$	$(0.40\pm0.10)\times10^{-11}$	$(0.33\pm0.10)\times10^{-11}$
E_a	0.9 ± 0.1	4.6 ± 0.2	5.8 ± 0.2
Experimental[c]			
A	$(1.4\pm0.3)\times10^{-10}$	$(0.9\pm2.4)\times10^{-11}$	$(2.0\pm2.9)\times10^{-11}$
E_a	1.2 ± 0.2	5.4 ± 1.9	7.2 ± 0.1

[a]Units are: k/cm^3 molecule^{-1} s^{-1}, A/cm^3 molecule^{-1} s^{-1}, and E_a/kcal mol^{-1}.
[b]For Cl+HCl and Cl+DCl k has been considered to be equal to 1/3 of $k(^2A')$, see the text.
[c]Experimental data for $H+Cl_2$ and Cl+HCl, DCl from Refs. 2 and 3 and 15, 16, and 18, respectively.
[d]Range of temperatures: $H+Cl_2$ (T: 252–730 K) and Cl+HCl, Cl+DCl (T: 312.5–423.2 K).

CD-SCSAG and ICVT/μOMT curves are very similar in the case of the PES of this contribution, but a strong difference between both data appears for the BCMR surface (see below). For our PES the ICVT/CD-SCSAG method yields the same results as the ICVT/μOMT one, and k(ICVT/μOMT)/k(ICVT) is equal to 1.13 and 1.05 at 300 and 500 K, respectively. The ratio k(ICVT/μOMT)/k(expt.) ranges from 1.04 to 1.52 in the 300–500 K temperature interval, while the ratio of Arrhenius parameters A(ICVT/μOMT)/A(expt.) and E_a(ICVT/μOMT)/E_a(expt.) are equal to 2.56 and 1.11, respectively. In what respects does the BCMR surface the ICVT/CD-SCSAG method yields very different results as compared to the ones of the ICVT/μOMT method. Thus, k(ICVT/μOMT)/k(ICVT) [k(ICVT/CD-SCSAG)/k(ICVT)] is equal to 15.48 (1.49) and 3.90 (1.16) at 300 and 500 K, respectively. This rather surprising enhancement of reactivity observed for the BCMR surface when passing from the CD-SCSAG to the μOMT tunneling correction is due to the shape of the minimum energy path in the vicinity of the saddle point. For the ICVT/μOMT method, the best VTST method considered in this work, the ratio k(ICVT/μOMT)/k(expt.) ranges from 1.76 to 1.06 in the 300–500 K temperature interval, while the ratio of Arrhenius parameters A(ICVT/μOMT)/A(expt.) and E_a(ICVT/μOMT)/E_a(expt.) are equal to 0.44 and 0.85, respectively. The direct comparison between the ICVT/μOMT data obtained with the PES derived here and the ones arising from the BCMR surface leads to: k(present PES)/k(BCMR) $=0.59-1.44$ from 300 to 500 K, A(present PES)/A(BMCR) $=5.75$, and E_a(present PES)/E_a(BCMR) $=1.30$. From the above-mentioned results it comes out that the BCMR surface describes a bit better the thermal rate constant of reaction (2), as it leads to E_a and A values that are, respectively, 15% and 56% lower than the corresponding experimental results,[15,16,18] while the PES derived here leads to E_a and A values that are, respectively, 11% and 156% higher than the experimental results, although the rate constant values are of similar quality when compared to measured data.

The quantum mechanical rate constant values for reaction (2) obtained using the CCH method and J-shifting approximation,[27] taking into account the three lowest PESs ($1\,^2A'$, $2\,^2A'$, and $1\,^2A''$) and both the electrostatic and spin–orbit coupling, are in excellent accord with experimental data[15,16,18] [Fig. 3(b)]. The main contribution to the rate constant arises from the $Cl(^2P_{3/2})+HCl \rightarrow HCl+Cl(^2P_{3/2})$ process (93% and 83% at $T=300$ and 1000 K, respectively). The MCSCF barrier for the ground PES has been scaled by 0.426[27] (value derived by trial and error using reactive scattering results) so as to reproduce the experimental rate constant. The results reported in Ref. 27 suggest that to perform an accurate calculation of the rate constant for reaction (2) it is necessary to include in the treatment the coupling between the three lowest PES, although only through the lowest one the system has enough energy to overcome the barrier and eventually reach the region of products.

There are two interesting possibilities in the context of the multisurface study reported in Ref. 27, to obtain a deeper insight on the Cl+HCl reaction. Thus, although those authors consider for comparison the single surface quantum

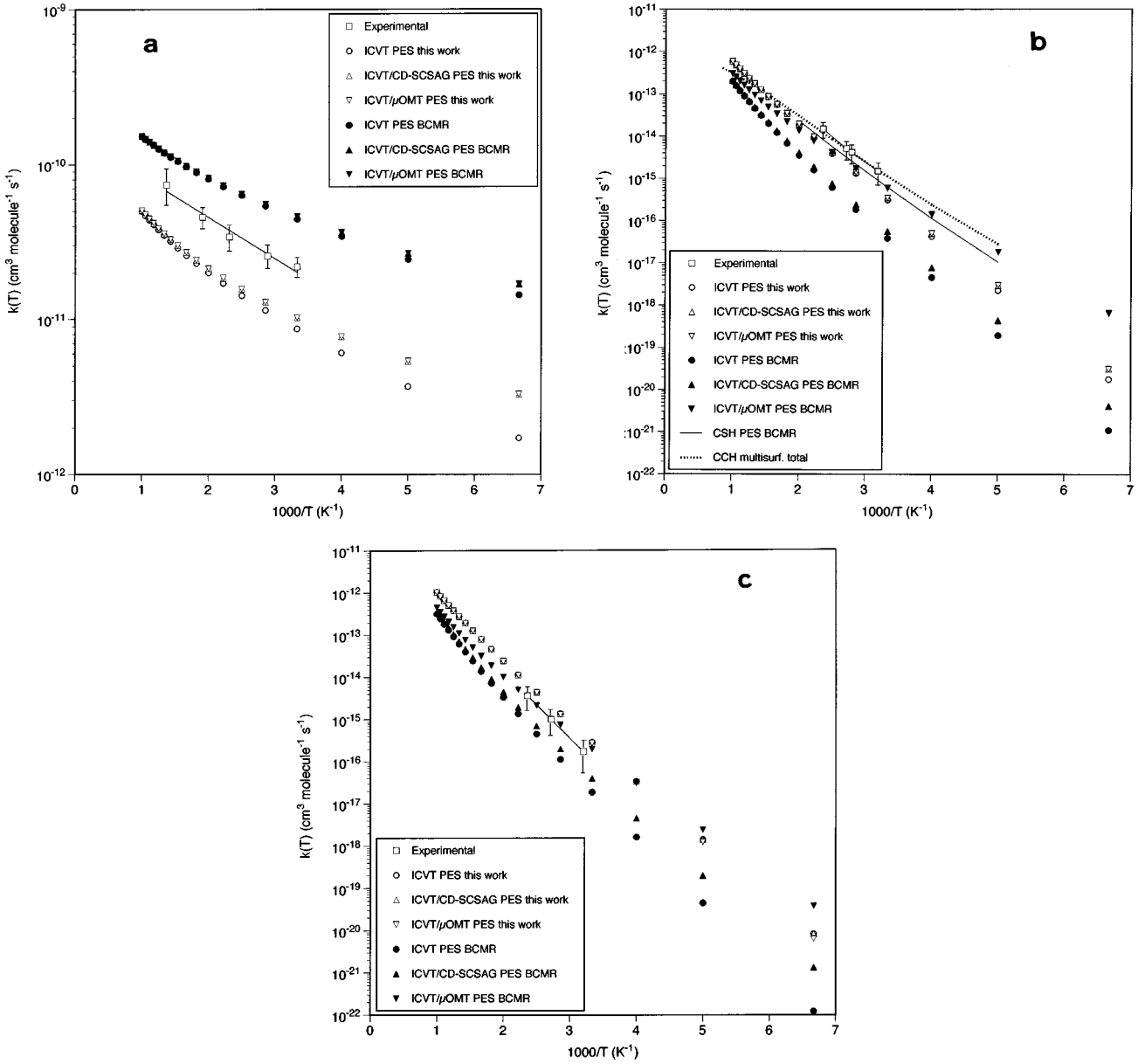

FIG. 3. Arrhenius plots of the variational transition state and experimental thermal rate constants: (a) $H+Cl_2 \rightarrow HCl+Cl$ reaction; (b) $Cl+HCl \rightarrow HCl+Cl$ reaction; (c) $Cl+DCl \rightarrow DCl+Cl$ reaction. For Cl+HCl, quantum mechanical rate constants at the single surface (BCMR PES) centrifugal sudden hyperspherical (CSH) (Ref. 24) and multisurface coupled-channel hyperspherical (CCH) (Ref. 27) levels are also shown (see the text).

mechanical scattering calculation that they performed at the CSH level using the BCMR PES[24] [see Fig. 3(b)], probably it would be useful to apply the same quantum mechanical method of Ref. 27 to the lowest PES including the energy correction due to the spin–orbit coupling. In this way, it would be possible to estimate the degree of adiabaticity that presents this system and its dependence with temperature. The second possibility refers to the multisurface study in the framework of the trajectory surface hopping (TSH) method, to obtain a picture of the way (degree of adiabaticity) the H atom transfer occurs. In this manner, it would be feasible to characterize the degree of adiabaticity of trajectories that are responsible for the different types of processes involved $[Cl(^2P_j)+HCl \rightarrow HCl+Cl(^2P_{j'})$, with $j=3/2 \rightarrow j'=3/2$, $j=3/2 \rightarrow j'=1/2$, $j=1/2 \rightarrow j'=3/2$, $j=1/2 \rightarrow j'=1/2]$.

For the Cl+DCl reaction the theoretical Arrhenius plots present a clear curvature, being valid here the same comments given for reaction (2). As for this reaction, the ICVT/CD-SCSAG and ICVT/μOMT curves are very similar in the case of the PES of this contribution, but a strong difference between both data appears for the BCMR surface. For our PES the ICVT/CD-SCSAG method yields quite close results as the ICVT/μOMT one [k(ICVT/μOMT)/k(ICVT/CD-SCSAG) is equal to 0.94 and 0.98 at 300 and 500 K, respectively), and k(ICVT/μOMT)/k(ICVT) is equal to 0.94 and 0.98 at 300 and 500 K, respectively. The ratio k(ICVT/μOMT)/k(expt.) ranges from 2.51 to 1.77 in the 300–500 K temperature interval, while the ratio of Arrhenius parameters A(ICVT/μOMT)/A(expt.) and E_a(ICVT/μOMT)/E_a(expt.) are equal to 0.95 and 0.93, respectively. In what respects to the BCMR surface the ICVT/CD-SCSAG method yields very different results as compared to the ones of the ICVT/μOMT method. Thus, k(ICVT/μOMT)/k(ICVT) [k(ICVT/CD-SCSAG)/

k(ICVT)] is equal to 10.37 (2.12) and 3.03 (1.32) at 300 and 500 K, respectively. For the ICVT/μOMT method, the ratio k(ICVT/μOMT)/k(expt.) ranges from 1.81 to 0.75 in the 300–500 K temperature interval, while the ratio of Arrhenius parameters A(ICVT/μOMT)/A(expt.) and E_a(ICVT/μOMT)/E_a(expt.) are equal to 0.17 and 0.81, respectively. The direct comparison between the ICVT/μOMT data obtained with the PES derived here and the ones arising from the BCMR surface leads to: k(present PES)/k(BCMR)$=1.38-2.35$ from 300 to 500 K, A(present PES)/A(BCMR)$=5.76$ and E_a(present PES)/E_a(BCMR)$=1.16$. From the above-mentioned results it comes out that our PES describes better the thermal rate constant of the Cl+DCl reaction, as it nearly quantitatively reproduces the experimental E_a (5% of error) and A (7% of error) values, while the BCMR surface leads to E_a and A values that are, respectively, 19% and 84% lower than the corresponding experimental results.[15,16,18]

IV. CONCLUDING REMARKS

In this work we have studied at an *ab initio* level the lowest potential energy surface (PES) of the HCl_2 system, which has $^2A'$ symmetry. This PES is the one involved in the $H(^2S)+Cl_2(X\ ^1\Sigma_g^+)\rightarrow HCl(X\ ^1\Sigma^+)+Cl(^2P)$ and $Cl(^2P)+HCl(X\ ^1\Sigma^+)\rightarrow HCl(X\ ^1\Sigma^+)+Cl(^2P)$ gas phase elementary chemical reactions. The former reaction is an important chemical laser while the second one is the most frequently used prototype of heavy–light–heavy (HLH) reaction. A large number of points on the $^2A'$ PES have been calculated at the PUMP2/6-311G($3d2f$,$3p2d$) level. The *ab initio* calculations show the existence of two angular transition states with negligible of very small barriers to collinearity. This and other properties of the PES are in agreement with previous studies. An analytical expression based on a many-body expansion has been used to obtain a satisfactory fit of the 740 *ab initio* points calculated, with a root-mean-square deviation within the range of the *ab initio* method error margin. This analytical representation of the $^2A'$ PES has been used to evaluate the variational transition state theory (VTST) thermal rate constant of the above-mentioned reactions, including tunneling corrections, and taken into account also the Cl+DCl system, obtaining quite good agreement when comparing with experimental rate constants. The analytical PES obtained in this work is suitable to be used in studies on the kinetics and dynamics of the HCl_2 system.

The reaction dynamics of these systems is being investigated in our group using the quasiclassical trajectory method and approximate quantum mechanical methods, employing the analytical PES developed in this work. We hope to report these results in the close future.

ACKNOWLEDGMENTS

This work has been supported by the ''Dirección General de Enseñanza Superior'' of the Spanish Ministry of Education and Culture (M.E.C.) through Project Nos. PB92-0756 and PB95-0598-C02-01. J.H. thanks the M.E.C. of Spain for a ''Formación de Profesorado Universitario'' Research Grant. The authors are also grateful to the ''Center de Supercomputació de Catalunya (CESCA)'' for supporting part of the computer time, and to Professor George C. Schatz (Northwestern University, USA) for sending us the quantum mechanical rate constant values of the Cl+HCl reaction.

[1] K. P. Huber and G. Herzberg, *Molecular Spectra and Molecular Structure IV. Constants of Diatomic Molecules* (Van Nostrand, New York, 1979).
[2] H. Gg. Wagner, U. Welzbacher, and R. Zellner, Ber. Bunsenges. Phys. Chem. **80**, 902 (1976).
[3] P. P. Bemand and M. A. A. Clyne, J. Chem. Soc. Faraday Trans. II **73**, 394 (1977).
[4] M. A. Wickramaaratchi, D. W. Setser, B. Hildebrandt, B. Korbitzer, and H. Heydtmann, Chem. Phys. **84**, 105 (1984).
[5] B. Hildebrandt, H. Vanni, and H. Heydtmann, Chem. Phys. **84**, 125 (1984).
[6] P. A. Berg and J. J. Sloan, J. Chem. Phys. **100**, 1075 (1994).
[7] A. M. G. Ding, L. J. Kirsch, D. S. Perry, J. C. Polanyi, and J. L. Schreiber, Faraday Discuss. Chem. Soc. **55**, 252 (1973).
[8] H. Heydtmann (private communication).
[9] J. J. Sloan (private communication).
[10] K. G. Anlauf, D. S. Horne, R. G. Macdonald, J. C. Polanyi, and K. B. Woodall, J. Chem. Phys. **57**, 1561 (1972).
[11] J. D. McDonald, P. R. LeBreton, Y. T. Lee, and D. R. Herschbach, J. Chem. Phys. **56**, 769 (1972).
[12] R. A. Eades, T. H. Dunning, and D. A. Dixon, J. Chem. Phys. **75**, 2008 (1981).
[13] M. A. Vincent, J. N. L. Connor, M. S. Gordon, and G. C. Schatz, Chem. Phys. Lett. **203**, 415 (1993).
[14] L. Visscher and K. G. Dyall, Chem. Phys. Lett. **239**, 181 (1995).
[15] F. S. Klein, A. Persky, and R. E. Weston, J. Chem. Phys. **41**, 1799 (1964).
[16] M. Kneba and J. Wolfrum, J. Phys. Chem. **83**, 69 (1979).
[17] M. Kneba and J. Wolfrum, Annu. Rev. Phys. Chem. **31**, 47 (1980).
[18] B. C. Garrett, D. G. Truhlar, A. F. Wagner, and T. H. Dunning, J. Chem. Phys. **78**, 4400 (1983).
[19] R. B. Metz, A Weaver, S. E. Bradforth, T. N. Kitsopoulos, and D. M. Neumark, J. Phys. Chem. **94**, 1377 (1990).
[20] I. Last and M. Baer, J. Chem. Phys. **86**, 5534 (1987).
[21] A. Persky and H. Kornweitz, J. Phys. Chem. **91**, 5496 (1987).
[22] H. Kornweitz, M. Broida, and A. Persky, J. Phys. Chem. **93**, 251 (1989).
[23] G. C. Schatz, B. Amaee, and J. N. L. Connor, J. Chem. Phys. **93**, 5544 (1990).
[24] D. Sokolovski, J. N. L. Connor, and G. C. Schatz, Chem. Phys. **207**, 461 (1996).
[25] G. C. Schatz, D. Sokolovski, and J. N. L. Connor, in *Advances in Molecular Vibrations and Collision Dynamics*, edited by J. M. Bowman (JAI Press, Greenwich, CT, 1994), Vol. 2B, p. 1.
[26] G. C. Schatz, J. Phys. Chem. **99**, 7522 (1995).
[27] C. S. Maierle, G. C. Schatz, M. S. Gordon, P. McCabe, and J. N. L. Connor, J. Chem. Soc. Faraday Trans. **93**, 709 (1997).
[28] D. K. Bondi, J. N. L. Connor, J. Manz, and J. Römelt, Mol. Phys. **50**, 467 (1983).
[29] GAUSSIAN-94, Revision B3, M. J. Frish, G. W. Trucks, M. Head-Gordon, P. M. W Gill, M. W. Wong, J. B. Foresman, B. G. Johnson, H. B. Schlegel, M. A. Robb, E. S. Replogle, R. Gomperts, J. L. Andres, K. Raghavachari, J. S. Binkley, C. González, R. L. Martin, D. J. Fox, D. J. Defrees, J. Baker, J. J. P. Stewart, and J. A. Pople, Gaussian, Inc., Pittsburgh, PA (1994).
[30] C. González and H. B. Schlegel, J. Phys. Chem. **90**, 2154 (1989).
[31] J. N. Murrell, S. Carter, S. C. Farantos, P. Huxley, and A. J. C. Varandas, *Molecular Potential Energy Surfaces* (Wiley, New York, 1984).
[32] M. González and R. Sayós, DIATOMFIT (unpublished program).
[33] R. Sayós and M. González, SM3FIT (unpublished program).
[34] M. González, J. Hijazo, J. J. Novoa, and R. Sayós, J. Chem. Phys. **105**, 10999 (1996).
[35] R. Steckler, W. Hu, Y. Liu, G. C. Lynch, B. C. Garrett, A. D. Isaacson, D. Lu, V. S. Melissas, T. N. Truong, S. N. Rai, G. C. Hancock, J. G. Lauderdale, T. Joseph, and D. G. Truhlar, Department of Chemistry and Supercomputer Institute, University of Minnesota, Minneapolis, MN 55455, POLYRATE program, version 6.5 (1995).